

## Luminescent spectroscopy of phosphates doped with Pr<sup>3+</sup> ions, irradiated with fast electrons and reactor neutrons

© S.A. Kiselev<sup>1</sup>, V.A. Pustovarov<sup>1</sup>, E.S. Trofimova<sup>1,2</sup>, M.O. Petrova<sup>3</sup>

<sup>1</sup> Ural Federal University after the first President of Russia B.N. Yeltsin, Yekaterinburg, Russia

<sup>2</sup> Skobeltsyn Institute of Nuclear Physics, Moscow State University,  
119991 Moscow, Russia

<sup>3</sup> Joint Institute for Nuclear Research, Moscow oblast, Dubna, Russia

e-mail: sviat-kiselev@yandex.ru

Received November 01, 2022

Revised January 10, 2023

Accepted February 06, 2023

This paper reports the spectroscopic properties of phosphates KLuP<sub>2</sub>O<sub>7</sub>, Sr<sub>9</sub>Sc(PO<sub>4</sub>)<sub>7</sub>, K<sub>3</sub>Lu(PO<sub>4</sub>)<sub>2</sub>, doped with Pr<sup>3+</sup> ions. Photoluminescence (PL) spectra under selective excitation with UV photons, PL excitation spectra, and decay kinetics of pulsed cathodoluminescence are studied. Recordings of luminescence spectra were done with non-irradiated samples and after their irradiation with fast electrons ( $E = 10$  MeV) or fast reactor neutrons. Three typical channels of electronic excitations radiative relaxation have been identified: interconfigurational  $d-f$  transitions, intraconfigurational  $d-f$  transitions in Pr<sup>3+</sup> ions and luminescence associated with defects. After irradiation, significant changes in the luminescence characteristics were observed: a redistribution of the intensity of the intraconfigurational  $f-f$  transitions, an increase in the luminescence yield of defects and the manifestation of new emission centers. The formation of radiation-induced defects presumably occurs due to the formation of complexes consisting of phosphorus and oxygen atoms.

**Keywords:** phosphates, luminescence,  $d-f$ -transitions,  $f-f$ -transitions, energy transfer, radiation-induced defects.

DOI: 10.61011/EOS.2023.05.56507.62-22

### Introduction

At the study of new scintillation materials, much attention is paid to inorganic compounds doped with rare-earth ions (REI), due to the potential diversity of their applications in various fields, such as detector systems, medical tomography, nuclear physics, etc. etc. Most of the REI luminescence properties are determined by intra- and interconfigurational emission transitions. Emission transitions  $5d-4f$  in the Pr<sup>3+</sup> ion in various matrices appear when a sufficiently strong crystal field shifts the lowest excited state  $4f^15d^1$  below the ground state  $^1S_0$  of the basic electronic configuration  $4f^2$  [1]. Three types of radiation are usually observed in scintillators based on phosphates, borates, and silicates doped with Pr<sup>3+</sup> ions: interconfigurational  $d-f$  transitions located in the UV range (250–320 nm), intraconfigurational  $f-f$  transitions (lines predominantly in the visible spectral range), and luminescence associated with defects [2,3]. Impurity Ce<sup>3+</sup> ions are now more often used in scintillation practice, but compounds with an admixture of Pr<sup>3+</sup> ions have a shorter decay time, and the emission spectrum is localized in the shorter wavelength region of the spectrum. Compared to impurity Ce<sup>3+</sup> ions, the decay kinetics of interconfigurational  $d-f$  transitions in Pr<sup>3+</sup> ions is characterized by a decay time of 20–30 ns instead of 30–60 ns for Ce<sup>3+</sup> ions [4–9].

The study of the modification of the optical and electrophysical properties of dielectrics and semiconductors

by high-energy particle fluxes is a practically important task. In most cases, such irradiation causes predominantly negative effects, such as a decrease in light output, structural changes, local amorphization, etc. Samples under study — KLuP<sub>2</sub>O<sub>7</sub>, Sr<sub>9</sub>Sc(PO<sub>4</sub>)<sub>7</sub>, K<sub>3</sub>Lu(PO<sub>4</sub>)<sub>2</sub> doped with Pr<sup>3+</sup> ions have already been proposed as potential scintillation materials with fast  $d-f$  transitions with an average decay time of 15–20 ns in the spectral region 250–300 nm [10,11]. Irradiation with an electron beam or a neutron flux, as expected, should affect the optical properties of these samples. The main effect of irradiation is the formation of point defects, which form a competing channel for radiative or nonradiative relaxation of electronic excitations due to energy transfer from impurity ions.

The aim of the work was to experimentally investigate, using luminescence spectroscopy methods, the properties of the above phosphates doped with Pr<sup>3+</sup> ions after their irradiation with fast electrons or fast neutrons in the channel of a nuclear reactor.

### 1. Objects and details of the experiment

Polycrystalline samples of KLuP<sub>2</sub>O<sub>7</sub>, Sr<sub>9</sub>Sc(PO<sub>4</sub>)<sub>7</sub>, K<sub>3</sub>Lu(PO<sub>4</sub>)<sub>2</sub> doped with Pr<sup>3+</sup> ions were synthesized by the solid-phase method and certified by X-ray diffraction at the Laboratory of Luminescent Materials of the University of Verona (Italy).

**KLuP<sub>2</sub>O<sub>7</sub> (1% Pr<sup>3+</sup>)**. The powder microcrystalline material has the composition KLu<sub>0.99</sub>Pr<sub>0.01</sub>P<sub>2</sub>O<sub>7</sub>, i.e. contains 1 mol% of Pr<sup>3+</sup> ions replacing Lu<sup>3+</sup> ions at the crystal lattice sites. High purity initial materials KNO<sub>3</sub>, (NH<sub>4</sub>)<sub>2</sub>HPO<sub>4</sub>, Lu<sub>2</sub>O<sub>3</sub> and Pr<sub>6</sub>O<sub>11</sub> (last two 4N reagents) were mixed and heat treated in a horizontal oven in air for 1 h at 400°C and 24 h at 750°C with intermediate regrinding. The phase purity of the prepared sample was examined by powder X-ray diffraction (PXRD) using a Thermo ARL XTRA powder diffractometer operating in the Bragg–Brentano geometry and equipped with an X-ray source with a copper anode ( $K\alpha$ ,  $\lambda = 1.5418 \text{ \AA}$ ) with a Si(Li)-cooled solid-state detector. The resulting PXRD template was fully compatible with the ICDD card № 01-076-7386 [10,12].

**Sr<sub>9</sub>Se(PO<sub>4</sub>)<sub>7</sub> (1% Pr<sup>3+</sup>)**. The PXRD analysis shows a perfect match with the JCPDS reference data, indicating the presence of a single-phase structure, as detailed in [13].

**K<sub>3</sub>Lu(PO<sub>4</sub>)<sub>2</sub> (1 and 5% Pr<sup>3+</sup>)**. Powders K<sub>2</sub>CO<sub>3</sub> (99%), (NH<sub>4</sub>)<sub>2</sub>HPO<sub>4</sub> (> 99%), Lu<sub>2</sub>O<sub>3</sub> (Aldrich, 99.99%) and Pr<sub>6</sub>O<sub>11</sub> (Aldrich, 99.999%) were mixed and pressed into granules under load 10 t. The samples were subjected to two heat treatments in air (600°C for 4 h and 950°C for 1 h) with intermediate grinding. At room temperature, this compound crystallizes into a structure with a trigonal unit cell belonging to the  $\bar{P}3$  space group. For this base material, two phase transitions are known to occur at lower temperatures around 250 and 140 K [9,11,14,15]. All diffraction peaks in the X-ray diffraction pattern of the K<sub>3</sub>Lu(PO<sub>4</sub>)<sub>2</sub>, doped 1% Pr<sup>3+</sup>, are consistent with the ICDD data of trigonal K<sub>3</sub>Lu(PO<sub>4</sub>)<sub>2</sub> (see Refs [11,16] for details).

Experimental results were obtained using various techniques. The photoluminescence (PL) and PL excitation spectra upon excitation in the UV range (from 3.5 to 5.8 eV) at room temperature were measured at the Laboratory of Solid State Physics of the Ural Federal University. Luminescence was excited using a DDS-400 deuterium lamp and a LOMO DMR-4 double prism monochromator. The PL spectra were detected using a DMR-4 double monochromator and a Hamamatsu R6358-10 photomultiplier. The presented PL spectra are not corrected for the spectral sensitivity of the detection system. The PL excitation spectra were normalized to an equal number of excitation photons using yellow lumogen, the quantum efficiency of which does not depend on the energy of excitation photons in the spectral area under study.

Low-temperature PL spectra (in the range 5–310 K) were measured using a HORIBA iXR320 spectrometer with a cooled CCD camera and an ozone-free Xe lamp. The PL excitation spectra were corrected for an equal number of exciting photons using a photodiode. The PL was measured using a closed-cycle cryostat (Cryo Trade Engineering, Moscow) with an RDK-20502 cryohead (Japan). A semiconductor diode with a Lake Shore controller was used to control and maintain the temperature of the samples.

Irradiation with fast electrons ( $E = 10 \text{ MeV}$ ) was carried out on a linear accelerator UELR-10-10S2 at the Ural

Federal University, Yekaterinburg. To avoid heating of the samples under the action of the beam, the existing conveyor system with portioned irradiation doses  $D = 11 \text{ kGy/cycle}$  was used. Using this system, the samples were irradiated for 4 s, then they moved around the conveyor for approximately 30 min. The absorbed dose was monitored using certified film dosimeters SO PDE-1/50 VNIIFTRI. Although the readings of the film dosimeter correspond to the absorbed dose  $D = 11 \text{ kGy/cycle}$ , our calculations using the Bethe formula and the Kanaya-Okayama [17] empirical formula for linear energy loss and maximum electron range give the dose value  $D = 4.3 \text{ kGy/cycle}$ . The total dose of electron irradiation of the samples accumulated over 15 and 30 cycles.

Neutron irradiation was carried out in the channel of the IBR-2 nuclear reactor at the Joint Institute for Nuclear Research, Dubna. Measurements of the fast neutron flux density ( $E > 1 \text{ MeV}$ ) were carried out by neutron activation analysis using a nickel satellite. For this analysis, a Canberra GC10021 laboratory  $\gamma$ -spectrometer and a Lynx multichannel analyzer were used. The flux density was  $3 \cdot 10^5 \text{ n/(cm}^2\text{s)}$ , fluence  $7 \cdot 10^{10} \text{ n/cm}^{-2}$ . The absorbed dose was determined using FWT-60-00 radiochromic dosimeters containing pararosaniline cyanide leuco dye in a nylon matrix and an FWT-92D photometer from Far West Technology, Inc. [18].

The decay kinetics of pulsed cathodoluminescence (PCL) was measured at the Laboratory of Solid State Physics of the Ural Federal University. As an excitation source, a pulsed small-sized electron accelerator MIRA-2D was used ( $E = 120 \text{ keV}$ , duration  $\sim 25 \text{ ns}$ ). The PCL kinetics were recorded using a DMR-4 double monochromator using an R6358-10 photomultiplier tube and a Tektronix TDS-2002 digital oscilloscope connected to a PC.

## 2. Results and discussion

### 2.1. PL under UV excitation

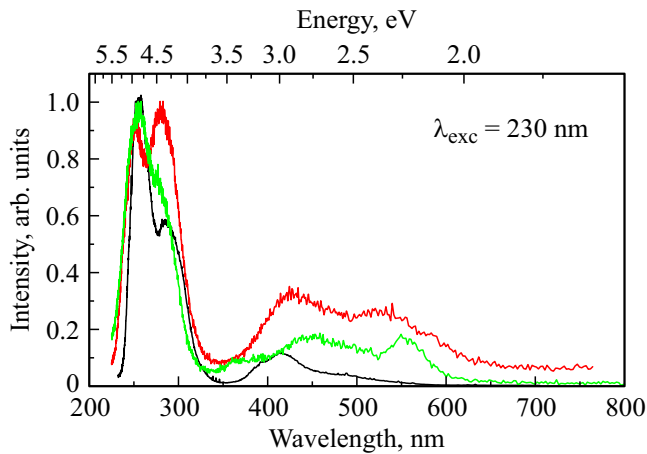
The results of measurements of the KLuP<sub>2</sub>O<sub>7</sub>:Pr<sup>3+</sup> (1%) PL are shown in Figs 1 and 2. Fig. 1 contains the spectra of samples before and after irradiation with fast electrons, the measurements were carried out at room temperature. It is clearly seen that irradiation causes significant changes in the form of the spectra. The broad UV bands dominating the PL spectra correspond to parity-allowed interconfigurational emission transitions from the lowest excited  $4f^15d^1$  state to multiplets of the ground electronic configuration  $4f^2$  of Pr<sup>3+</sup> ion. There are almost no lines of intraconfigurational radiative  $f-f$  transitions. Photoluminescence associated with defects is represented by a wide band in the range from 350 to 600 nm with a maximum at approximately 450 nm.

In the PL spectra of the irradiated samples, a redistribution of the intensity of the bands of interconfigurational transitions should be noted. The behavior of PL associated with defects changes more sharply. The non-irradiated sample shows one (maximum at 415 nm) band with low

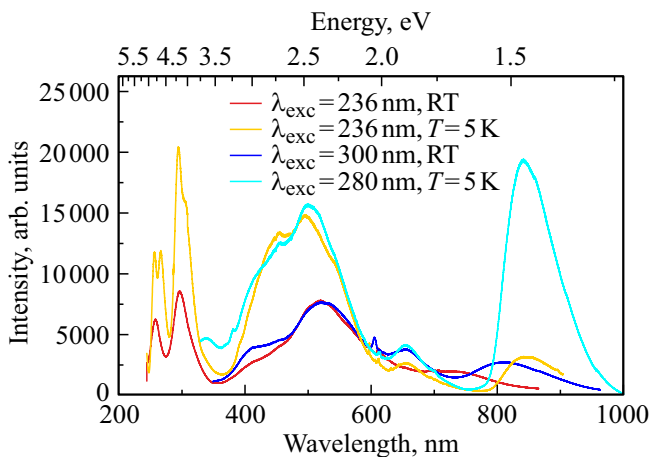
relative intensity, after irradiation the shape of this band becomes more complex — separation into two peaks (425 and 540 nm) is observed. Upon further irradiation with a higher dose, the defective luminescence is still represented by two bands at 460 and 580 nm, and the latter dominates in the PL spectrum.

Fig. 2 shows the PL spectra of neutron-irradiated samples measured at room temperature (RT) and  $T = 5$  K. At different energies of exciting photons, there are four main bands: 440, 520, 650, and 840 nm. It should be noted that a new long-wavelength band with a maximum at 840 nm is clearly distinguished, which is effectively excited in the region of 280 nm at low temperatures.

The PL spectrum shown in Fig. 3 demonstrates the complex structure of the PL band in the area of 520 nm. Here, against the background of a broad defect emission band, there are narrow lines of intraconfigurational  $f-f$



**Figure 1.** PL spectra of  $\text{KLuP}_2\text{O}_7:\text{Pr}^{3+}$  (1%) under UV excitation ( $\lambda_{\text{exc}}$ ),  $T = 295$  K before (black) and after irradiation with electrons with an energy of 10 MeV (green — 15 cycles, red — 30 cycles).



**Figure 2.** PL spectra of  $\text{KLuP}_2\text{O}_7:\text{Pr}^{3+}$  (1%) under UV excitation ( $\lambda_{\text{exc}}$ ),  $T = 5$  and 295 K (RT) before (red, blue) and after neutron irradiation (orange, blue).

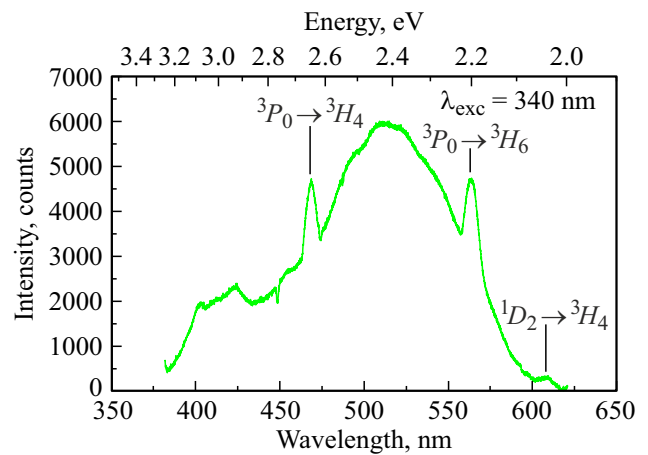


**Figure 3.** PL spectrum  $\text{KLuP}_2\text{O}_7:\text{Pr}^{3+}$  (1%), irradiated with fast neutrons,  $\lambda_{\text{exc}} = 340$  nm,  $T = 5$  K.

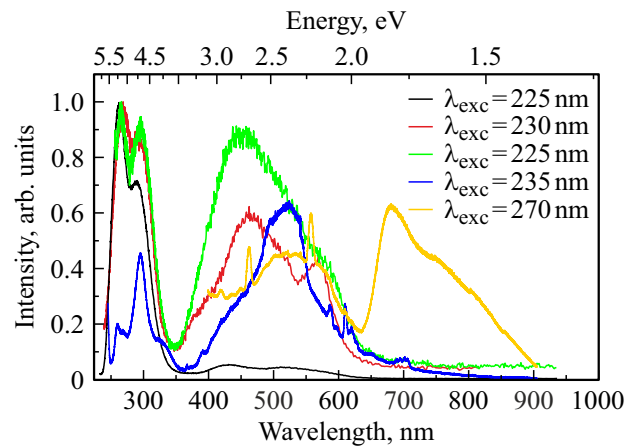


**Figure 4.** PL spectra of  $\text{Sr}_9\text{Sc}(\text{PO}_4)_7:\text{Pr}^{3+}$  (1%) under UV excitation ( $\lambda_{\text{exc}}$ ),  $T = 295$  K before (black) and after irradiation with electrons (red — 15 cycles, green — 30 cycles) and neutrons (blue, orange).

transitions, but their yield is low compared to  $d-f$  transitions. This situation is typical for compounds in which the Stokes shift of interconfigurational transitions does not exceed 0.4 eV [1]. As previously calculated [10], for  $\text{KLuP}_2\text{O}_7:\text{Pr}^{3+}$  the Stokes shift of  $d-f$  luminescence does not exceed 0.38 eV. Nevertheless, in Fig. 3 one can observe the appearance of narrow lines of the  $f-f$  transitions.

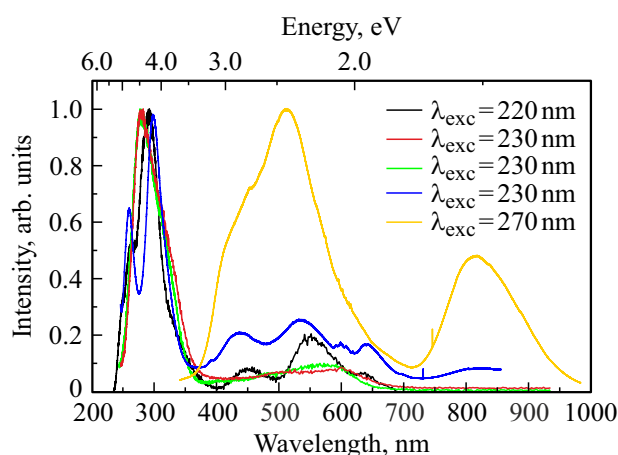
PL spectra of  $\text{Sr}_9\text{Sc}(\text{PO}_4)_7:\text{Pr}^{3+}$  (1%) are shown in Fig. 4. In the non-irradiated sample, the UV bands of the  $d-f$  transitions dominate in the PL spectra, the defect bands are weakly pronounced, and intraconfigurational  $f-f$  transitions are hardly observed.

After irradiation with fast electrons, there is a redistribution of the intensity of the bands of the  $d-f$  transitions and a decrease in their yield. Most likely, this behavior is due to the creation of an alternative channel for the relaxation of the excited states of praseodymium ions due to the transfer of energy to defects. The behavior of defect-

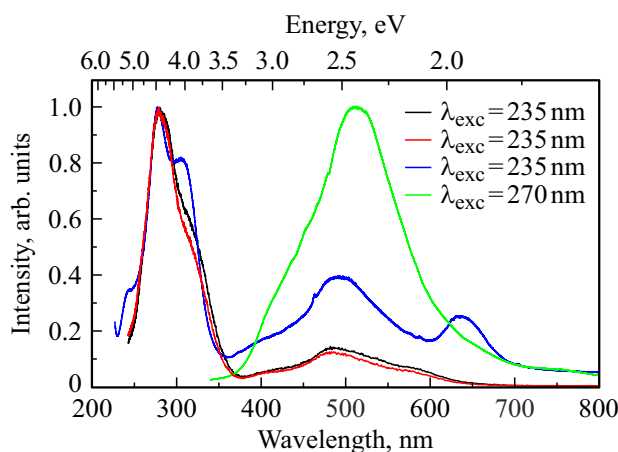
related luminescence is a more interesting problem. First, after irradiation, there is an increase in the yield of the band associated with the PL of defects in comparison with the unirradiated sample. Thus, it can be seen that there is an effective mechanism for the radiation formation of defects, presumably based on the radical groups of phosphorus and oxygen. Second, in the case of electron irradiation, the dependence of the intensity of defective bands on the absorbed dose is noticeable. The spectrum indicated by the red line corresponds to the dose of 70 kGy, and the green line — to the dose of 140 kGy. It is clearly seen that the PL band associated with the defect becomes more intense and the intensity of the observed bands is redistributed. After irradiation with both electrons and neutrons, the emerging PL bands of defects have similar maxima at 450 and 540 nm. The PL spectrum after irradiation with neutrons upon excitation by 270 nm photons shows a complex band structure similar to that shown in Fig. 3, and additionally, there is a new asymmetric emission band with a maximum at approximately 680 nm.

Fig. 5, 6 show the PL spectra of K<sub>3</sub>Lu(PO<sub>4</sub>)<sub>2</sub>:Pr<sup>3+</sup> (1 and 5%). The relative intensity of *d*–*f* transitions increases above the level of defective luminescence in the case of electron irradiation, but after neutron irradiation the spectrum changes much more significantly. Both the 1% and 5% samples contain luminescence bands associated with defects. At 1% concentration level of Pr<sup>3+</sup> ions, this band has two separated peaks with maxima at 450 and 550 nm, and at 5% — one band 490 nm. In the K<sub>3</sub>Lu(PO<sub>4</sub>)<sub>2</sub>:Pr<sup>3+</sup> (5%) sample, there is also a band with a maximum in the area of 650 nm — similar to that observed in the neutron-irradiated KLuP<sub>2</sub>O<sub>7</sub>:Pr<sup>3+</sup> (1%), Fig. 2.

Based on a comparison of the presented PL spectra and literature data [19–24], an assumption about the structure of the observed defects can be made. The crystal structure of the studied phosphates contains [PO<sub>4</sub>] tetrahedral complexes; therefore, defects should be expected similar to those in glassy SiO<sub>2</sub> [21,22]. Such defects are formed when the phosphorus-oxygen bond is broken with the formation of a radical (PO<sub>4</sub>)<sup>2-</sup> (defects of the P1 type according to the classification [19,20]), a non-bridging oxygen atom, or the formation of oxygen-deficient centers. Let us note that the radicals (PO<sub>4</sub>)<sup>2-</sup> are characteristic point defects of a number of complex phosphate compounds [19,20,23,24]. However, it is known [21,22] that, as in SiO<sub>2</sub>, the radical (PO<sub>4</sub>)<sup>2-</sup> cannot be stabilized in a regular crystal structure. The formation of stable defects suggests its local amorphization after irradiation. On the other hand, a comparison of the recorded PL spectra and PL excitation correlates well with the data presented in [19] on defects of the P4 type, which correspond to the radical (PO<sub>2</sub>)<sup>2-</sup>, which appears when the bonds between the phosphorus atom and two oxygen atoms in the tetrahedral structure [PO<sub>4</sub>] are broken. This type of defects is well manifested in the EPR spectra [20], the measurement of which for the samples under study is



**Figure 5.** PL spectra of K<sub>3</sub>Lu(PO<sub>4</sub>)<sub>2</sub>:Pr<sup>3+</sup> (1%) under UV excitation ( $\lambda_{\text{exc}}$ ),  $T = 295$  K before (black) and after irradiation with electrons (green — 15 cycles, red — 30 cycles) and neutrons (blue, orange).



**Figure 6.** PL spectra of K<sub>3</sub>Lu(PO<sub>4</sub>)<sub>2</sub>:Pr<sup>3+</sup> (5%) under UV excitation ( $\lambda_{\text{exc}}$ ),  $T = 295$  K before (black) and after irradiation with electrons (red) and neutrons (blue, green).

necessary to confirm the proposed assumption about the defect structure.

## 2.2. PL excitation

The PL excitation spectra of the irradiated KLuP<sub>2</sub>O<sub>7</sub>:Pr<sup>3+</sup> (1%) samples recorded in different emission bands ( $E_{\text{emis}}$ ) are shown in Fig. 7 and 8. There are excitation features associated with intracenter transitions  $4f^{15}d^1 \rightarrow 4f^2$  in Pr<sup>3+</sup> ions as a broad complex band in the far UV area. The excitation spectrum measured for the 450 nm band shows a slight increase near 5 eV, followed by a further increase in the excitation efficiency in the high-energy area up to the limiting energy of 6.0 eV. Photoluminescence of defects and  $4f^{15}d^1 \rightarrow 4f^2$  emission are excited in almost the same spectral area. This indicates that there is an effective transfer of

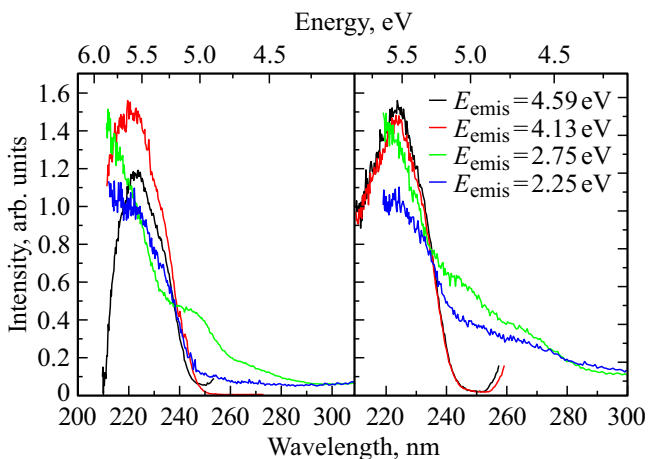


**Figure 7.** PL excitation spectra of  $\text{KLuP}_2\text{O}_7:\text{Pr}^{3+}$  (1%),  $T = 295$  K before (left) and after electron irradiation (right).

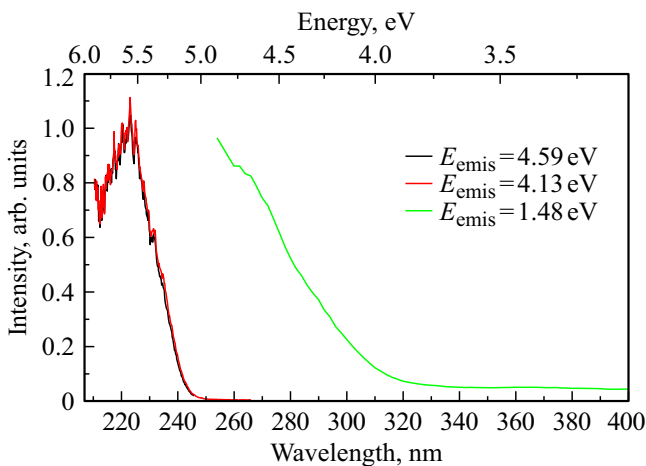


**Figure 8.** PL excitation spectra of  $\text{KLuP}_2\text{O}_7:\text{Pr}^{3+}$  (1%),  $T = 295$  K after neutron irradiation.

energy from impurity centers to defects in the crystal lattice, i.e., crystal lattice defects form an alternative channel for the relaxation of excited states of ions  $\text{Pr}^{3+}$ .

The PL excitation spectra of another phosphate  $\text{K}_3\text{Lu}(\text{PO}_4)_2:\text{Pr}^{3+}$  (1 and 5%) before and after irradiation with electrons or neutrons are shown in Fig. 9, 10. All spectra are dominated by broad bands in the area above 5.0 eV. The excitation spectra given for  $E_{\text{emis}} = 4.56$  eV correspond to intracenter interconfigurational transitions  $4f^2 \rightarrow 4f^15d^1$  in  $\text{Pr}^{3+}$  ions. As can be seen, in the PL excitation spectra of defects ( $E_{\text{emis}} = 2.09$  eV) of irradiated samples, the highest excitation efficiency is observed in the same spectral range as for interconfigurational transitions. This fact confirms the conclusion that the defects of the crystal lattice, which appear in the PL spectra in the visible range, act as a competing channel for the relaxation of the excited states of the  $\text{Pr}^{3+}$  ions. However, it should be noted that the excitation spectra measured for the

PL bands of defects at energies of 1.55 eV and 1.88 eV contain a dominant band in the area of 4.7 eV, which correlates with the literature data for the PL of non-bridging oxygen atoms in  $\text{SiO}_2$  [21,22] and suggests the PL manifestation of such defects in the samples under study.

The PL excitation spectra of  $\text{Sr}_9\text{Sc}(\text{PO}_4)_7:\text{Pr}^{3+}$  (1%) for interconfigurational transitions and defects ( $E_{\text{emis}} = 2.15$  eV) are characterized similarly to the above discussions for the  $\text{K}_3\text{Lu}(\text{PO}_4)_2:\text{Pr}^{3+}$  samples (Fig. 11). There is also energy transfer from impurity centers to crystal lattice defects. The excitation spectrum for the PL band associated with defects at  $E_{\text{emis}} = 1.82$  eV (Fig. 11) has a pronounced additional maximum at 2.75 eV. The lack of literature data for this compound precludes correlation with other studies.

### 2.3. Temperature dependence of defect luminescence

For interconfigurational  $4f^15d^1 \rightarrow 4f^2$  transitions in the studied phosphates, the temperature dependence of the X-ray luminescence yield is given and discussed in papers [10,11]. Fig. 12 for  $\text{KLuP}_2\text{O}_7:\text{Pr}^{3+}$  (1%) irradiated with neutrons shows the temperature dependence of the PL associated with defects. There is an increase in the PL yield upon cooling. The PL intensity is practically independent of temperature in the range 5–20 K; at room temperature, the PL yield drops to approximately 0.15 of the initial value. The temperature dependence is satisfactorily approximated by the Mott formula, as shown by the solid line in Fig. 12 (insert):

$$I(T) = I_0 / \left( 1 + A \exp\left(-\frac{\varepsilon_a}{k_B T}\right) \right), \quad (1)$$

where  $A$  — constant,  $k_B$  — Boltzmann constant,  $\varepsilon_a$  — thermal activation energy. The results of the approximation give the value of the activation energy  $\varepsilon_a \sim 0.035$  eV. Another parameter that is often used to describe thermal quenching is the characteristic quenching temperature  $T_Q$ , which corresponds to the temperature at which the PL yield is halved. As follows from the results presented in Fig. 12, the characteristic quenching temperature for PL defects in  $\text{KLuP}_2\text{O}_7:\text{Pr}^{3+}$  is  $T_Q = 140$  K.

### 2.4. Pulsed cathodoluminescence decay kinetics

The luminescence decay kinetics of interconfigurational  $4f^15d^1 \rightarrow 4f^2$  transitions in the studied phosphates has been studied in detail under pulsed laser excitation by UV photons, X-ray synchrotron radiation, or an electron beam [10–14,16]. The characteristic decay time of  $4f^15d^1 \rightarrow 4f^2$  emission in  $\text{Pr}^{3+}$  ions in phosphates was 17–20 ns. In this section we study pulsed cathodoluminescence decay kinetics for samples irradiated with fast neutrons. The pulsed cathodoluminescence (PCL) decay

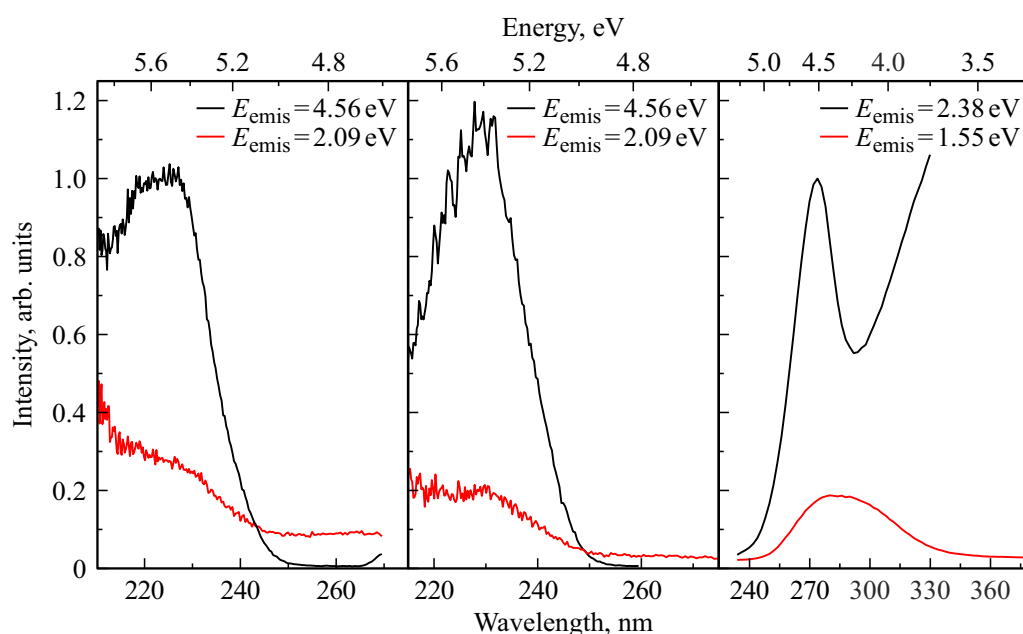


**Figure 9.** PL excitation spectra of  $K_3Lu(PO_4)_2:Pr^{3+}$  (1%),  $T = 295$  K before (left) and after irradiation with electrons (center) and neutrons (right).

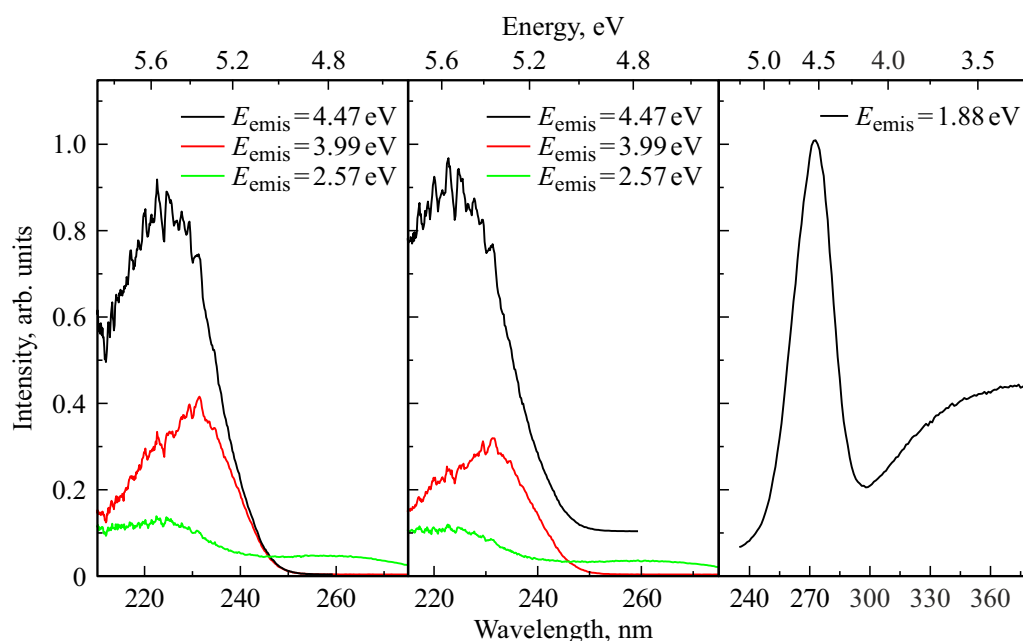


**Figure 10.** PL excitation spectra of  $K_3Lu(PO_4)_2:Pr^{3+}$  (5%),  $T = 295$  K before (left) and after irradiation with electrons (center) and neutrons (right).

kinetics for the samples under study are shown in Fig. 13. It should be emphasized that in most cases they are well approximated by the multi-exponential approximation:

$$I(t) = \sum A_i \exp\left(-\frac{t}{\tau_i}\right) + I_0, \quad (2)$$

where  $I_0$  — the contribution of the slow components of the decay kinetics, forming the so-called „pedestal“;

$A_i$  — amplitudes of each exponential component;  $\tau_i$  — exponential decay time. For each sample, based on the presented PL spectra, the main luminescence bands were selected, the maxima of which are designated  $\lambda_{emis}$ . Most of the emission bands at room temperature are characterized by the main component of PCL decay with time in the range  $\sim 40$ – $70$  ns. The contribution of the  $\mu$ s-band components practically does not exceed 10%. The short PCL decay



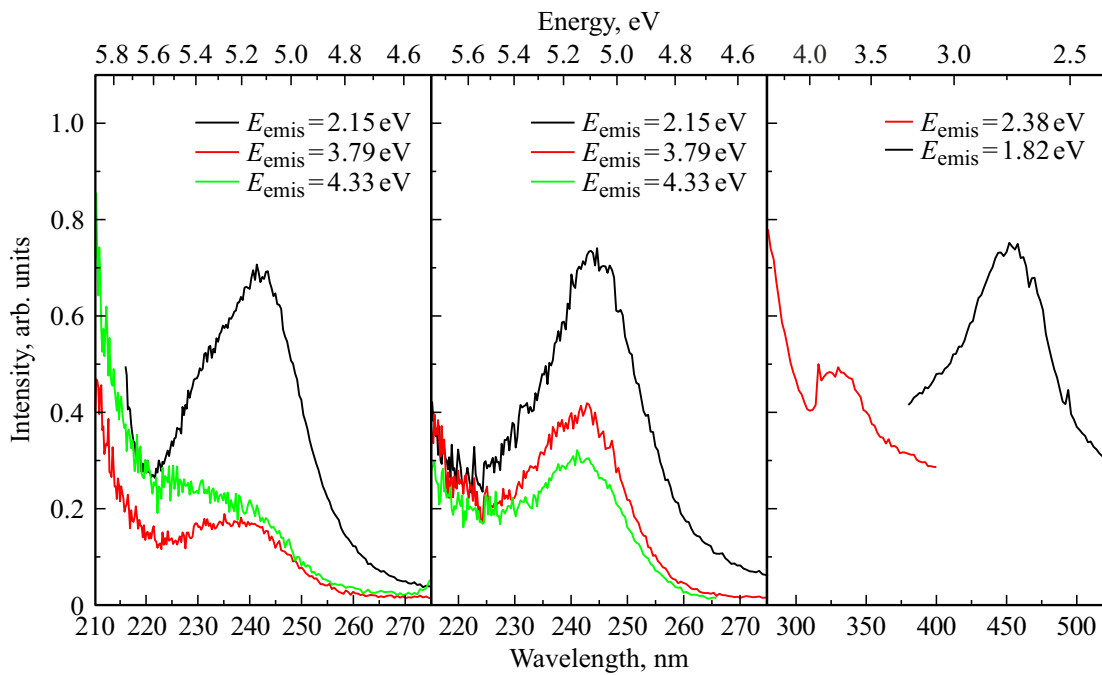


**Figure 11.** PL excitation spectra of  $\text{Sr}_9\text{Sc}(\text{PO}_4)_7:\text{Pr}^{3+}(1\%)$ ,  $T = 295\text{ K}$  before (left) and after irradiation with electrons (center) and neutrons (right).

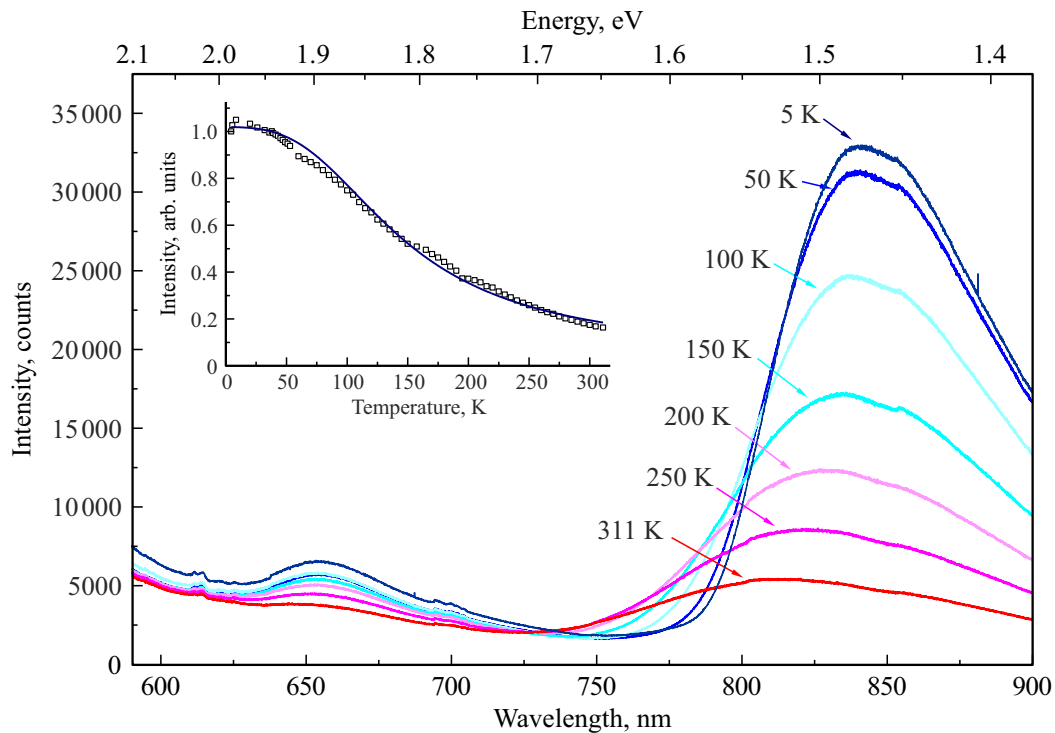


**Figure 12.** PL spectra  $\text{KLuP}_2\text{O}_7:\text{Pr}^{3+}(1\%)$  after irradiation with neutrons under UV excitation ( $\lambda_{\text{exc}} = 280\text{ nm}$ ), measured at different temperatures. Inset: temperature dependence of the intensity of the 840 nm PL band (circles) and its approximation by the Mott formula (solid line).

time indicates the manifestation of singlet-triplet transitions in emission centers; however, this may also reflect the processes of temperature quenching of luminescence, as

follows from the results presented above in Section 2.3. The results of approximation of the PCL decay kinetics for different emission bands are presented in the table.

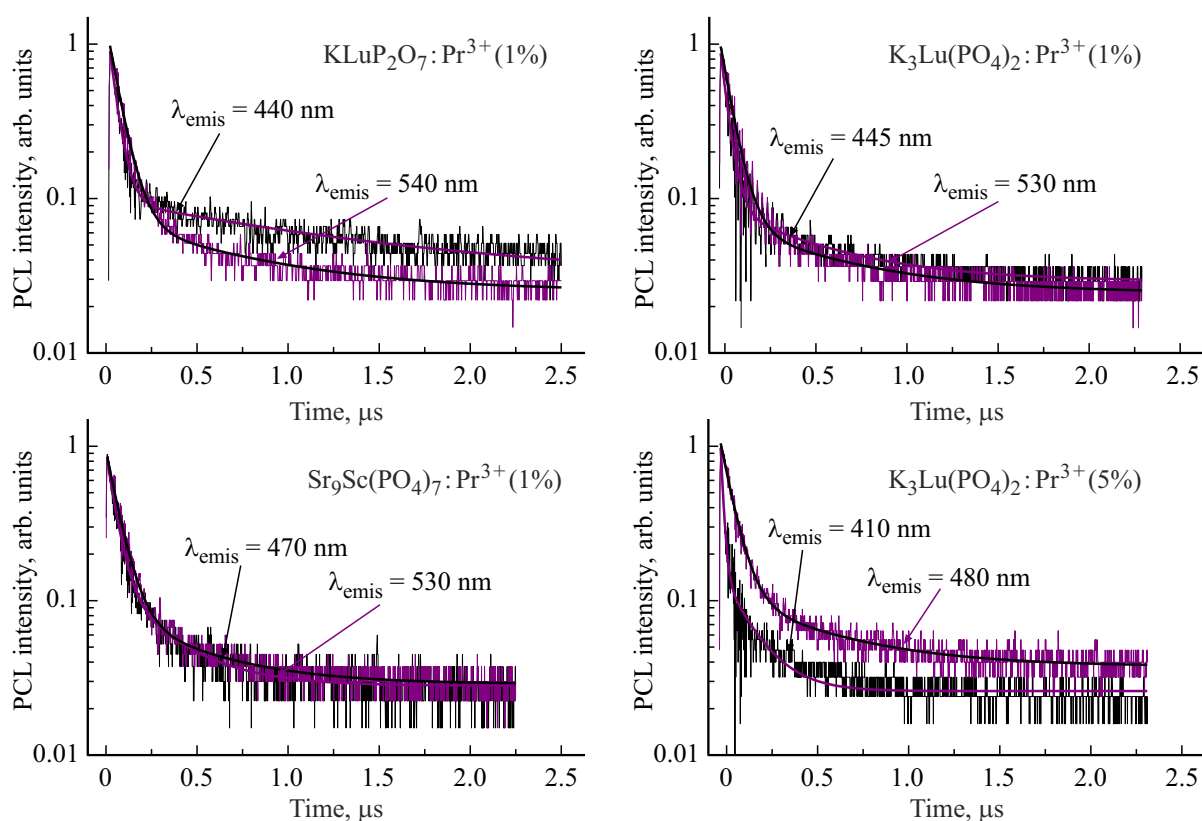


**Figure 13.** PCL decay kinetics for samples irradiated with fast neutrons. Solid lines — result of approximation using approximation (2),  $T = 295$  K.

Approximation results of PCL decay kinetics

	KLuP <sub>2</sub> O <sub>7</sub> :Pr <sup>3+</sup> (1%)		K <sub>3</sub> Lu(PO <sub>4</sub> ) <sub>2</sub> :Pr <sup>3+</sup> (1%)		K <sub>3</sub> Lu(PO <sub>4</sub> ) <sub>2</sub> :Pr <sup>3+</sup> (5%)		Sr <sub>9</sub> Sc(PO <sub>4</sub> ) <sub>7</sub> :Pr <sup>3+</sup> (1%)	
	440 nm	540 nm	445 nm	530 nm	410 nm	480 nm	470 nm	530 nm
$\tau_1$ , ns	42	64	40	61	45	67	51	67
$\tau_2$ , μs	1.3	0.7	0.5	0.6	0.2	0.5	0.3	0.5
$I_0$	0.10	0.05	0.07	0.05	0.03	0.08	0.04	0.05
$A_1$	1.01	1.01	1.05	1.02	1.05	1.03	1.01	1.02
$A_2$	0.15	0.07	0.06	0.08	0.08	0.11	0.06	0.08

## Conclusion

The paper presents the results of luminescence studies of KLuP<sub>2</sub>O<sub>7</sub>, K<sub>3</sub>Lu(PO<sub>4</sub>)<sub>2</sub>, Sr<sub>9</sub>Sc(PO<sub>4</sub>)<sub>7</sub>) micropowders doped with Pr<sup>3+</sup> ions before and after their irradiation with fast electrons or fast neutrons in the channel of a nuclear reactor. The PL spectra of unirradiated samples are dominated by fast interconfigurational radiative  $4f^15d^1 \rightarrow 4f^2$  transitions in Pr<sup>3+</sup> ions. Due to the small value of the Stokes shift, the contribution of intraconfigurational transitions of  $4f^2 \rightarrow 4f^2$  is very small.

After irradiation, significant changes are found in the form of the PL spectra. First, there is a redistribution of the intensity of the bands of interconfigurational transitions. This behavior is due to the creation of an alternative channel for the relaxation of the excited states of praseodymium

ions due to the transfer of energy to defects. Second, the contribution of luminescence associated with defects and forming low-energy broad emission bands increases in proportion to the fluence. Thus, irradiation with fast electrons or neutrons is an effective way to create radiation-induced defects by the mechanism of impact displacement and breaking of intermolecular bonds. As the PL excitation spectra show, the luminescence of defects is effectively excited in the same spectral region as the interconfigurational  $4f^15d^1 \rightarrow 4f^2$  emission of Pr<sup>3+</sup> ions. This indicates an efficient nonradiative energy transfer from the excited states of the impurity ion to the defects. An alternative channel for the relaxation of the excited states of the impurity ion is formed.

The decay kinetics of PCL associated with defect emission at room temperature exhibits a two-exponential be-



havior described by two main components ( $\tau_1 \sim 40\text{--}60$  ns and  $\tau_2 \sim 0.5\text{--}1.3$   $\mu$ s). The short PCL decay time indicates the manifestation of singlet-triplet transitions in emission centers; however, this may also reflect the processes of temperature quenching of luminescence. The PL intensity of defects decreases as the temperature increases from 5 K according to the Mott law. The calculated quenching temperature  $T_Q$  for the dominant 850 nm band in the PL spectra in  ${}_2\text{O}_7\text{:Pr}^{3+}$  (1%) was 140 K.

Based on a comparison of the literature and experimental spectroscopic data on defects in the studied phosphates, it can be assumed that stable radicals based on phosphorus-oxygen complexes are formed after irradiation. Their stabilization suggests local amorphization of the crystal lattice. To confirm the proposed assumption, additional EPR studies are required.

## Funding

This paper was financially supported by the Ministry of Science and Higher Education of the Russian Federation (basic part of the state assignment, project № FEUZ-2023-0013) and the Development Program of the Ural Federal University within the framework of the „Priority-2030“ Program. The authors thank Prof. M. Bettinelli (Laboratory of Luminescent Materials, University of Verona, Italy) for providing samples for research and fruitful collaboration.

## Conflict of interest

The authors declare that they have no conflict of interest.

## References

- [1] A.M. Srivastava. *J. Lumin.*, **169**, 445 (2016). DOI: 10.1016/j.jlumin.2015.07.001
- [2] V. Gorbenko, E. Zych, T. Voznyak, S. Nizankovskiy, T. Zorenko, Yu. Zorenko. *Opt. Mater.*, **66**, 271 (2017). DOI: 10.1016/j.optmat.2017.02.00
- [3] N. Kristianpoller, D. Weiss, N. Khaidukov, V.N. Makhov, R. Chen. *Rad. Meas.*, **43** (2), 245 (2008). DOI: 10.1016/j.radmeas.2007.11.001
- [4] M. Nikl, V.V. Laguta, A. Vedda. *Phys. Status Solidi B*, **245**, 1701 (2008). DOI: 10.1002/pssb.200844039
- [5] M. Nikl, H. Ogino, A. Yoshikawa, E. Mihokova, J. Pejchal, A. Beitlerova, A. Novoselov, T. Fukuda. *Chem. Phys. Lett.*, **410**, 218 (2005). DOI: 10.1016/j.cplett.2005.04.115
- [6] I. Carrasco, K. Bartosiewicz, F. Piccinelli, M. Nikl, M. Bettinelli. *J. Lumin.*, **189**, 113 (2017). DOI: 10.1016/j.jlumin.2016.08.022
- [7] V.A. Pustovarov, A.N. Razumov, D.I. Vyprintsev. *Phys. Solid State*, **56**, 347 (2014). DOI: 10.1134/S1063783414020267
- [8] D. Wisniewski, A.J. Wojtowicz, W. Drozdowski, J.M. Farmer, L.A. Boatner. *J. Alloy Compd.*, **380**, 191 (2004). DOI: 10.1016/j.jallcom.2004.03.042
- [9] A. Zych, M. de Lange, C. d. M. Donega, A. Meijerink. *J. Appl. Phys.*, **112**, 013536 (2012). DOI: 10.1063/1.4731735
- [10] V.A. Pustovarov, K.V. Ivanovskikh, S.A. Kiselev, E.S. Trofimova, S. Omelkov, M. Bettinelli. *Opt. Mat.*, **108**, 110234 (2020). DOI: 10.1016/j.optmat.2020.110234
- [11] K.V. Ivanovskikh, V.A. Pustovarov, S. Omelkov, M. Kirm, F. Piccinelli, M. Bettinelli. *J. Lumin.*, **230**, 117749 (2021). DOI: 10.1016/j.jlumin.2020.117749
- [12] M. Trevisani, K. Ivanovskikh, F. Piccinelli, M. Bettinelli. *Zeitschrift fur Naturforschung B*, **69**, 205 (2014). DOI: 10.5560/znb.2014-3260
- [13] V.A. Pustovarov, K.V. Ivanovskikh, Yu.E. Khatchenko, V.Yu. Ivanov, M. Bettinelli, Q. Shi. *Phys. Solid State*, **61** (5), 867–871 (2019). DOI: 10.21883/FST.2019.05.47582.12F
- [14] V.A. Pustovarov, E.I. Zinin, A.L. Krymov, B.V. Shulgin. *Rev. Sci. Instrum.*, **63**, 3524 (1992). DOI: 10.1063/1.1143760
- [15] E. Radzhabov, V. Nagirnyi. In: *IOP Conf. Series: Mat. Sci. Eng.* (IOP Publishing, 2010), vol. 15 (1), p. 012029. DOI: 10.1088/1757-899X/15/1/012029
- [16] V.A. Pustovarov, K.V. Ivanovskikh, Yu.E. Khatchenko, V.Yu. Ivanov, M. Bettinelli, Q. Shi. *Phys. Solid State*, **61**, 758–762 (2019). DOI: 10.1134/S1063783419050275
- [17] K. Kanaya, S. Okayama. *J. Phys. D: Appl. Phys.*, **5** (1), 43 (1972). DOI: 10.1088/0022-3727/5/1/308
- [18] M.O. Petrova, M.V. Bulavin, A.D. Rogov, A. Yskakov, A.V. Galushko. *Instrum. Exp. Tech.*, **65**, 371 (2022). DOI: 10.1134/S0020441222030046
- [19] S. Girard, A. Alessi, N. Richard, L. Martin-Samos, V. de Michele. *Rev. Phys.*, **4**, 100032 (2019). DOI: 10.1016/j.revip.2019.100032
- [20] G. Origlio, F. Messina, M. Cannas, R. Boscaino, S. Girard, A. Boukenter, Y. Ouerdane. *Phys. Rev. B*, **80**, 205208 (2009). DOI: 10.1103/PhysRevB.80.205208
- [21] A.R. Silin, A.N. Trukhin. *Point defects and electronic excitations in crystalline and glassy SiO<sub>2</sub>* (Zinatne, Riga, 1985).
- [22] L. Skuja. *J. Non-Cryst. Solids*, **239** (1–3), 16 (1998). DOI: 10.1016/s0022-3093(98)00720-0
- [23] V.A. Pustovarov, A.F. Zatsepin, V.S. Cheremnykh, A.A. Syrtsov, S.O. Cholakh. *Radiat. Eff. Defects Solids*, **157** (6–12), 751 (2002). DOI: 10.1080/10420150215800
- [24] A.N. Sreeram, L.W. Hobbs, N. Bordes, R.C. Ewing. *Nucl. Instr. And Meth. B*, **116** (1–4), 126 (1996). DOI: 10.1016/0168-583X(96)00022-5

Translated by E.Potapova